Supporting Information

Self-healing strain sensors based on nanostructured supramolecular conductive elastomers

*Xuehui Liu, Canhui Lu, Xiaodong Wu and Xinxing Zhang**

State Key Laboratory of Polymer Materials Engineering, Polymer Research Institute of Sichuan University, Chengdu 610065, China.

*E-mail: xxzwwh@scu.edu.cn.

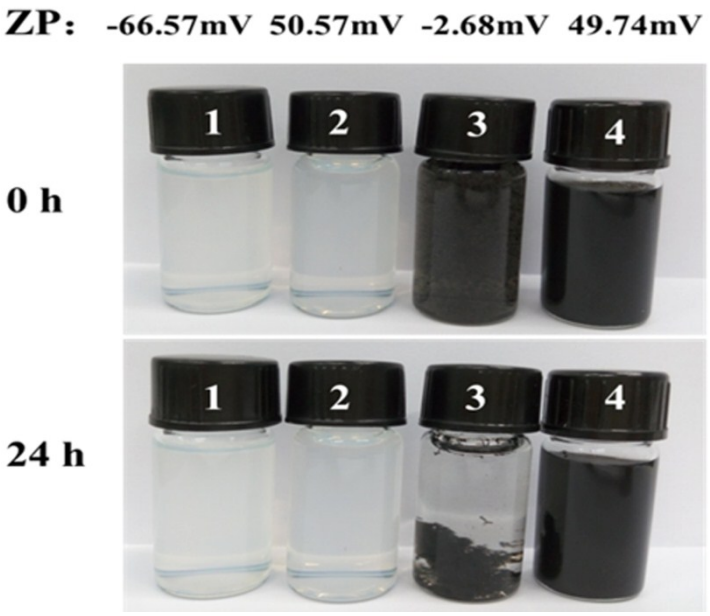

Fig. S1 Aqueous suspension properties and Zeta potential of (1) CNC, (2) PEI@CNC, (3) CNTs and (4) CNTs@(PEI@CNC) nanohybrids, respectively.

As shown in **Fig. S1**, the z-potential of CNC suspension is changed from -66.5 ± 1.0 mV to 50.5 ± 1.0 mV after modification with PEI, indicating that the PEI was successfully adsorbed on CNC surface. Furthermore, the PEI@CNC nanohybrid exhibits good suspension stability in water. In contrary, the neat CNT dispersion with a Zeta potential of -2.6 ± 1.0 mV shows poor suspension stability. After ultrasonically assisted mixing with PEI@CNC, the Zeta potential of CNTs@(PEI@CNC) was measured to be 49.7 ± 1.0 mV, indicating the good suspension stability. The CNTs @(PEI@CNC) suspension was still stable even after standing for 24 h, while the neat CNTs was agglomerated and precipitated. The results indicate that the PEI@CNC nanohybrids could effectively disperse neat CNTs to obtain homogeneous aqueous dispersion.

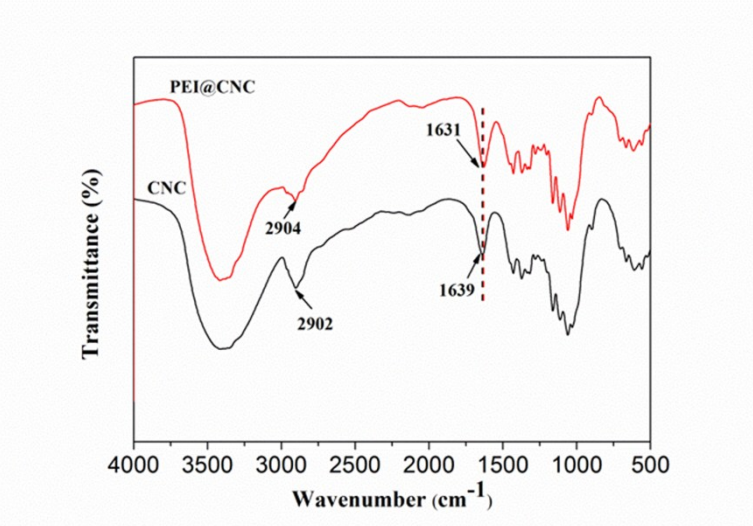

Fig. S2 FT-IR spectra of neat CNC and PEI@CNC nanohybrids.

The chemical structure of neat CNC and PEI-modified CNC was investigated by FT-IR spectroscopy as shown in Fig. S2. All the characteristic bands of CNC, e.g. 3413 cm^{-1} corresponding to O-H stretching, 2902 cm^{-1} corresponding to C-H stretching, and 1060-1162 cm^{-1} corresponding to C-O-C pyranose ring skeletal vibration, appear in the spectra of both CNC and PEI@CNC nanohybrids. The band at 2902 cm^{-1} becomes broader than that of neat CNC, while the band at 1639 cm^{-1} shifts to lower wavenumber after the modification by PEI. The FT-IR results further confirm that PEI was adsorbed onto the surface of CNC.

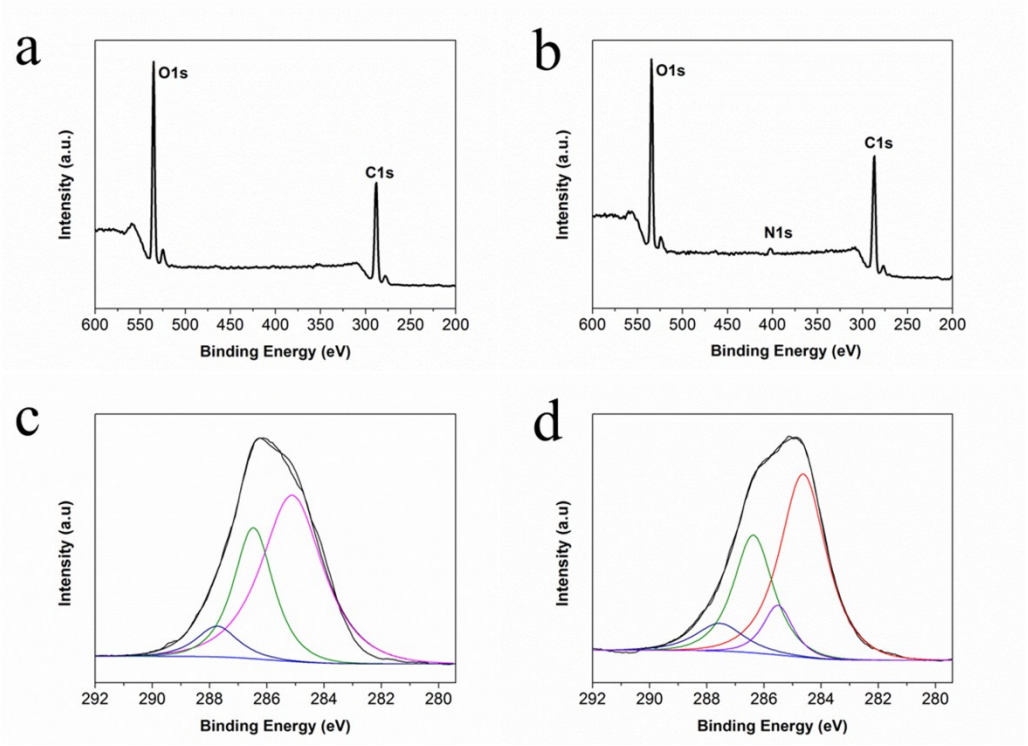

Fig. S3 Survey XPS spectra of neat CNC (a) and PEI@CNC nanohybrids (b); C 1s core-level spectra of neat CNC (c) and PEI@CNC nanohybrids (d).

To further demonstrate the adsorption of PEI on CNC, the neat CNC and PEI@CNC nanohybrids were further characterized by XPS analysis. As shown in **Fig. S3a**, the CNC spectrum shows peak components of C 1s and O 1s at binding energies of about 288 and 535 eV, which could be assigned to C and O elements in CNC, respectively. After the modification reaction, a new peak for N 1s at 402 eV was clearly observed in the spectrum of PEI@CNC nanohybrids (**Fig. S3**b), suggesting that there are considerable amount of nitrogen atoms in the structure due to the introduction of PEI into CNC. Moreover, the C 1s core-level spectra of CNC shows that carbon atom is present at three different chemical environments. The peaks at 287.7, 286.4, and 285.1 are ascribed to O-C-O/C=O, C-O, and C-C/C-H, respectively. After modification of CNC with PEI, a new peak appeared at 285.5 eV which could be attributed to C-N (**Fig. S3c, d**). The results indicate that PEI with abundant amine groups was adsorbed onto the surface of CNC.

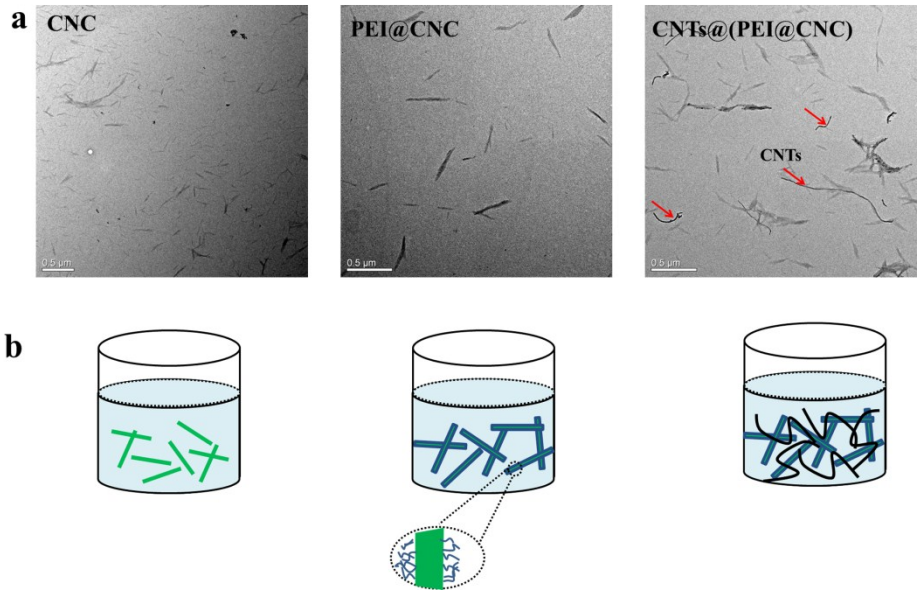

Fig. S4 TEM images of neat CNC, PEI@CNC, and CNTs@(PEI@CNC) nanohybrids.

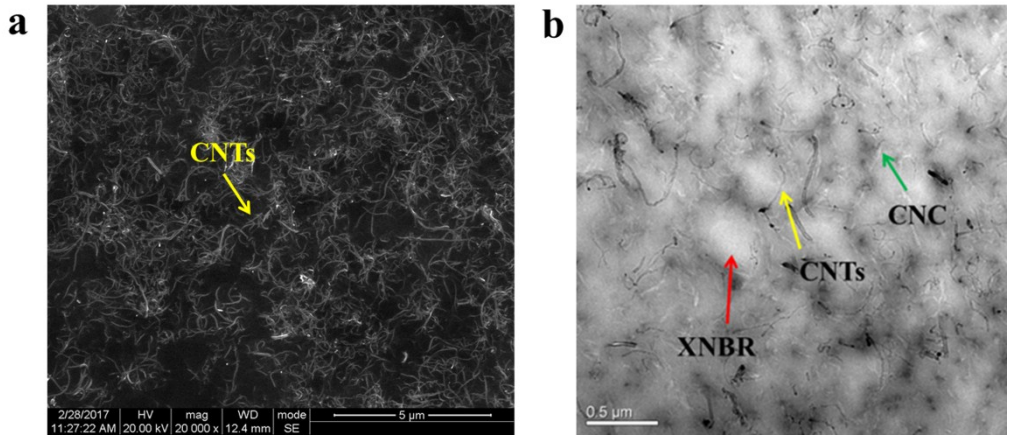

Fig. S5 SEM images of NSCE composites (a) and TEM images (b) of NSCE composites.

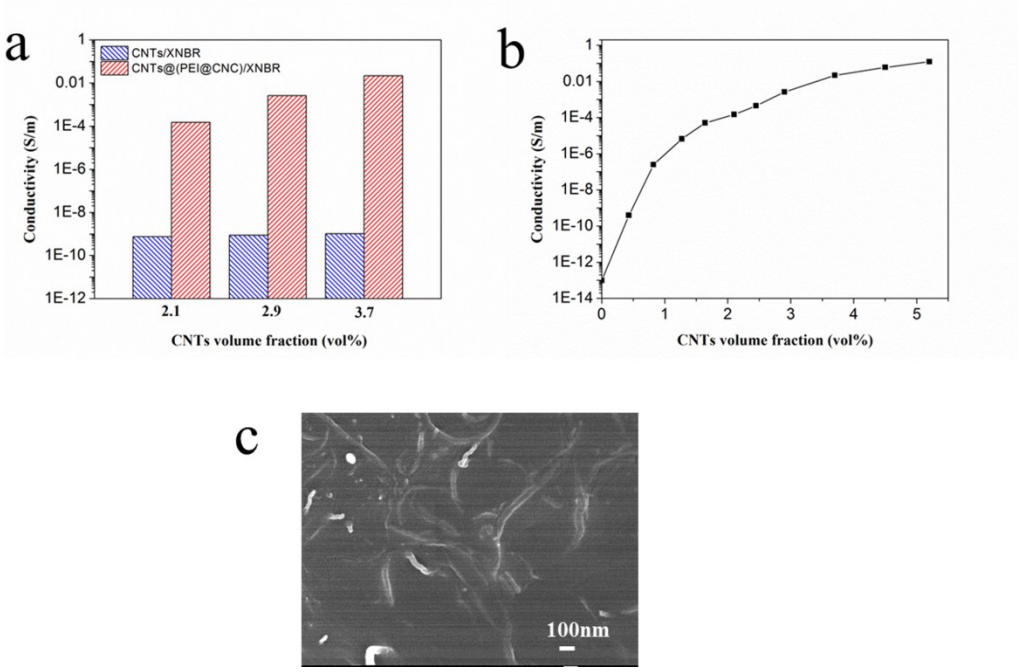

Fig. S6 Electrical conductivity comparison of the as-prepared NSCE composites and homogeneously dispersed CNTs/XNBR composites with different CNTs volume fractions (a); electrical conductivity of the as-prepared NSCE composites as a function of CNTs volume fraction (b); SEM image of CNTs@CNC/XNBR with CNTs content of 0.43 vol% (c).

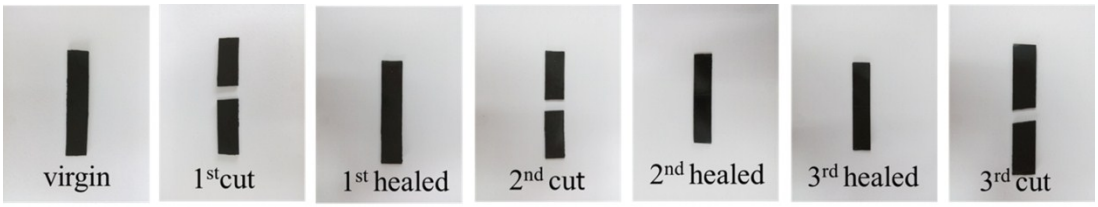

Fig. S7 Digital camera pictures of NSCE composites before and after three cutting/healing cycles at the same severed location.

In **Fig. S7**, the virgin sample of NSCE composites was first cut apart in the middle. After healing by hot-pressing at 160 ^{o}C for 10 min, the mended sample was cut again in the same severed location. It is apparent that the sample remained the virgin state without obvious damage after three cutting/healing cycles, which is attributed to the excellent self-healing ability of our NSCE composites.

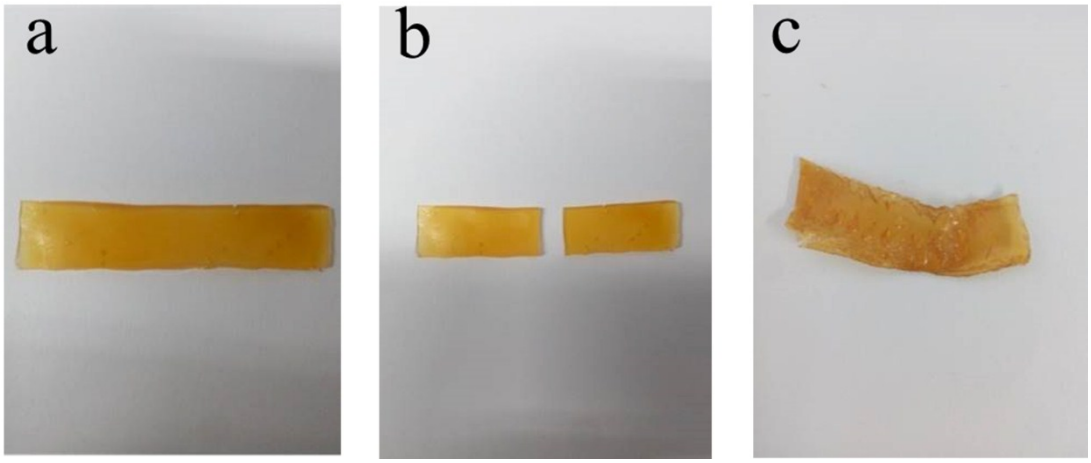

Fig. S8 Photographs of the self-healing performance of un-crosslinked XNBR. Virgin sample (a), completely cut sample (b), healed sample (c).

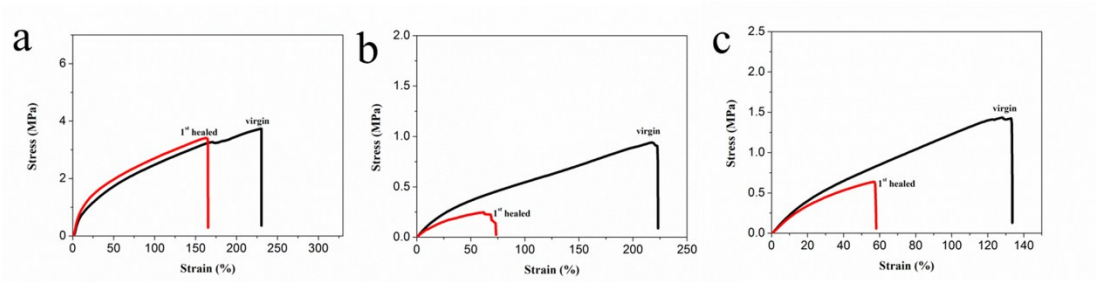

Fig. S9 Stress-strain curves of virgin and healed samples of nanostructured PEI@CNC/XNBR composites (a), un-crosslinked CNC/XNBR composites (b) and sulfur-crosslinked CNC/XNBR composites (c).

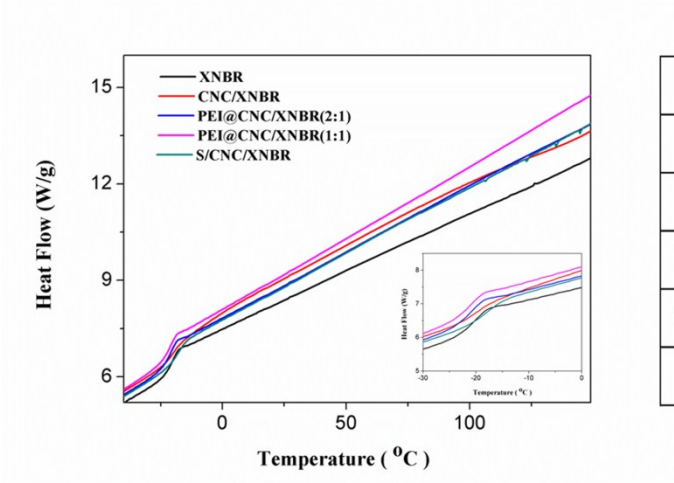

Composites	Tg(°C)
XNBR	-20.2
CNC/XNBR	-19.9
PEI@CNC/XNBR(2:1)	-21.3
PEI@CNC/XNBR(1:1)	-21.4
S/CNC/XNBR	-18.3

Fig. S10 Differential scanning calorimetric study of XNBR, CNC/XNBR, PEI@CNC (2:1)/XNBR composites, PEI@CNC(1:1)/XNBR composites and sulfur-crosslinked CNC/XNBR composites.

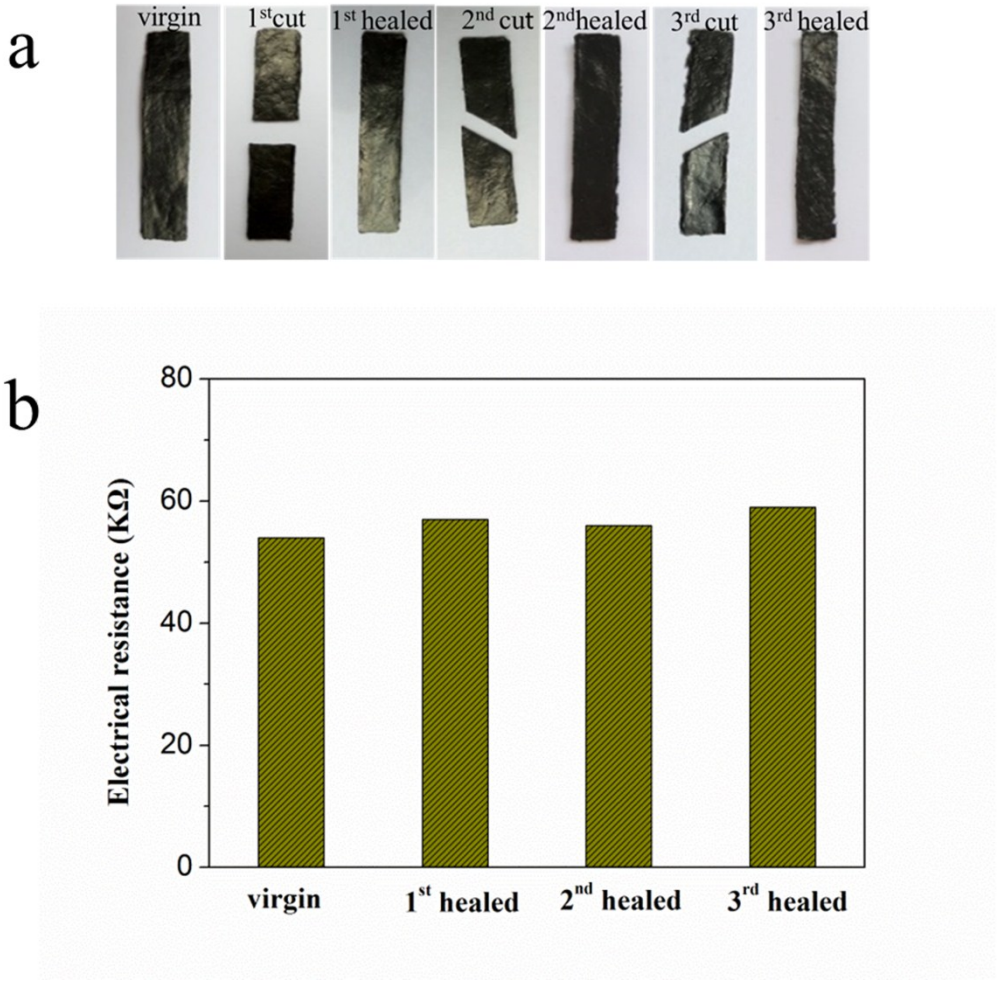

Fig. S11 Digital pictures (a) and electric resistance (b) of NSCE composites before and after three cutting/healing cycles at different severed location.

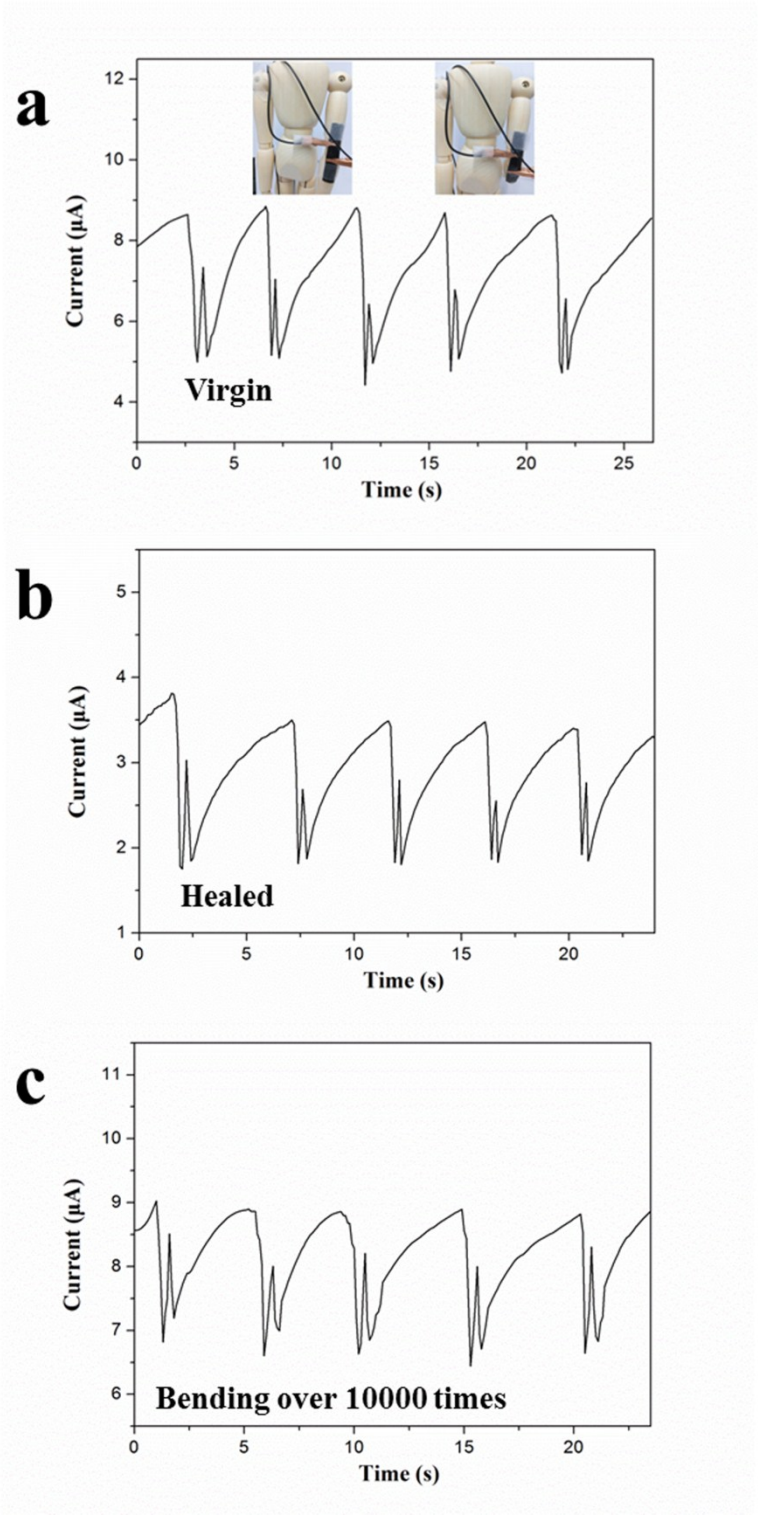

Fig. S12 Current responses of a sensor strip attached to the puppet's elbow (as inset picture shows) when bending and releasing. Virgin sensor strips (a), healed sensor strips (b), healed sensor strips bent over 10000 times (c).